Novel approaches to polymer blends based on polymer nanoparticles

THOMAS KIETZKE[1], DIETER NEHER*[1], KATHARINA LANDFESTER*[2], RIVELINO MONTENEGRO[2], ROLAND GÜNTNER[3] AND ULLRICH SCHERF*[3]

[1]University of Potsdam, Institute of Physics, Am Neuen Palais 10, D-14469 Potsdam, Germany
[2]Max Planck Institute of Colloids and Interfaces, D-14424 Potsdam/Golm, Germany
[3]University of Wuppertal, Department of Chemistry, Gaußstrasse 20, D-42097 Wuppertal, Germany
*e-mail: neher@rz.uni-potsdam.de; landfester@mpikg-golm.mpg.de; scherf@uni-wuppertal.de

Published online: 11 May 2003; doi:10.1038/nmat889

Polymer layers can exhibit significantly improved performances if they possess a multicomponent phase-separated morphology. We present two approaches to control the dimensions of phase separation in thin polymer-blend layers; both rely on polymer nanospheres prepared by the miniemulsion process. In the first approach, heterophase solid layers are prepared from an aqueous dispersion containing nanoparticles of two polymers, whereas in the second approach, both polymers are already contained in each individual nanoparticle. In both cases, the upper limit for the dimension of phase separation is determined by the size of the individual nanoparticles, which can be adjusted down to a few tens of nanometres. We also show that the efficiencies of solar cells using two-component particles are comparable to those of devices prepared from solution at comparable illumination conditions, and that they are not affected by the choice of solvent used in the miniemulsion process.

Solid blends of polymers can exhibit mechanical, optical and electro-optical properties not attainable with a single polymer, especially if the blend morphology is formed at submicrometre scales. Moreover, many biological, optical and electro-optical devices include thin layers of polymer blends, which are usually deposited from a solution of all polymer components in a common solvent. For example, highly efficient organic solar cells have been made from thin layers containing a blend of an electron-donating and an electron-accepting polymer[1–3]. In this case, the dimension of phase separation must be in the range of the exciton diffusion length, commonly a few tens of nanometres, and the overall layer thickness should not greatly exceed the penetration depth of the incident light.

However, because the entropy of mixing is generally low for polymers, solid polymer blends tend to phase-separate at the macroscopic scale. Moreover, when a thin layer of immiscible polymers is deposited from solution, the resulting morphology strongly depends on various parameters, such as the individual solubility of the polymers in the solvent used, the interaction with the substrate surface, the layer thickness and the method of deposition, drying and annealing[4–10]. Therefore, the adjustment of the lengths of phase separation in thin layers is often arbitrary and based on trial-and-error.

Several strategies have therefore been developed to form well-defined and predictable multicomponent polymer structures with phase-separation at the nanometre scale. The most straight-forward approach is to use linear block copolymers[11,12]. However, the drawback of this approach is that both components, A and B, with their different chemical and electronic structures, have to be connected by a covalent bond, which limits the availability of possible A–B pairs. In fact, only few examples of block copolymers containing two semiconducting polymers have been reported[13,14]. AB diblock copolymers have also been used as compatibilizers in bulk blends of the corresponding homopolymers A and B[15,16]. Finally, co-continuous nanostructured polymer morphologies have been prepared by reactive blending[17]; in this approach, one component bears reactive groups along the backbone and the second component possesses complementary reactive moieties only at one end. Even though this novel strategy is

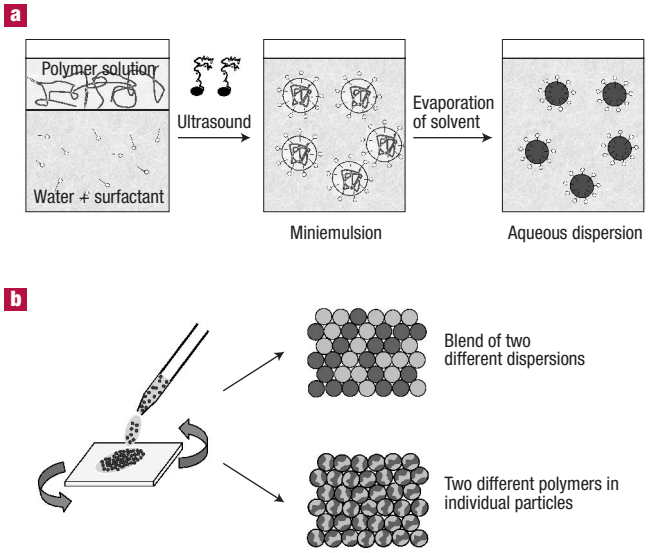

Figure 1 a, Preparation of a dispersion of solid polymer nanoparticles in water. First, a solution of the polymer in an organic solvent is mixed with water containing an appropriate surfactant. A miniemulsion is then formed on stirring and ultrasonication. Finally, the solvent is evaporated, resulting in solid polymer nanoparticles dispersed in water. **b**, Strategies to prepare binary polymer blends using polymer nanospheres. Phase-separated structures at the nanometre scale can be prepared either by coating a layer from a dispersion containing nanoparticles of two different polymers, or by using dispersions that contain both polymers in each individual nanoparticle.

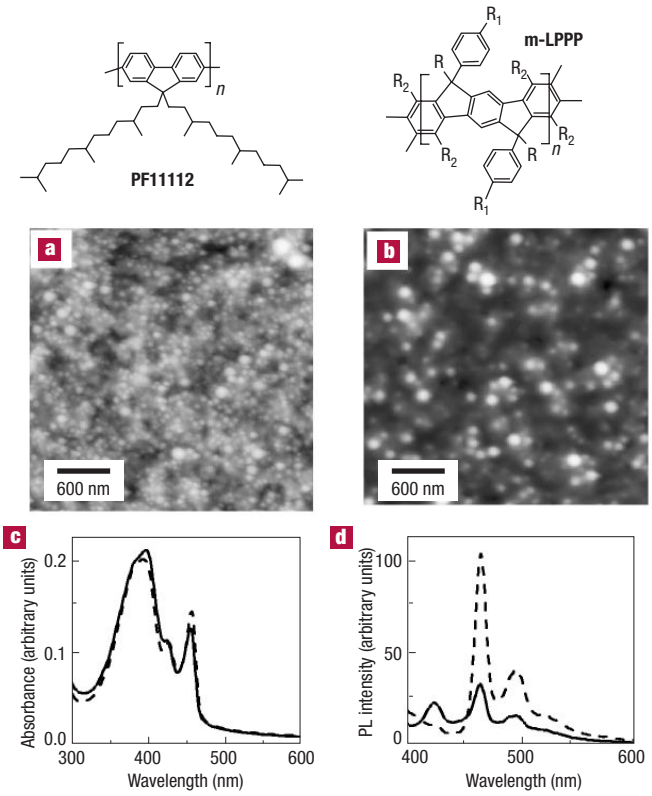

Figure 2 Morphology and energy transfer in layers of nanoparticle blends. a, **b**, Atomic force microscope (AFM) height images of a film prepared from a 1:1 mixture of particles of the low-T_g polymer PF11112 (diameter, $d = 75$ nm) and the high-T_g polymer m-LPPP ($d = 95$ nm), before annealing (**a**), and after annealing at 150 °C for 1 h in inert atmosphere (**b**). **c**, The absorption of the m-LPPP/PF11112 particle-blend layer measured before (solid line) and after annealing at 200 °C for 1 h (dashed line). **d**, The corresponding photoluminescence (PL) spectra, recorded for an excitation wavelength of 380 nm. Also depicted is the chemical structure of poly(9,9-bis(3,7,11-trimethyldodecyl)fluorene-2,7-diyl) (PF11112) and the ladder-type poly(*p*-phenylene) (m-LPPP). The substituents on m-LPPP are: R = methyl; R_1 = decyl and R_2 = hexyl.

expected to be versatile, it has yet to be proven that it is applicable to a wide range of polymers, including semiconducting or fluorescent materials, and that it can be used in thin layers.

We have demonstrated that aqueous dispersions containing nanospheres of various polymers can be produced by the miniemulsion process[18]. The polymer is first dissolved in a suitable solvent (which is not miscible with water) and added to an aqueous solution containing an appropriate surfactant (Fig. 1a). By applying high shear, for example, by ultrasonicating the mixture, stable miniemulsions containing small droplets of the polymer solution are obtained. Evaporation of the solvent finally results in a stable dispersion of solid polymer nanoparticles in water. We have further demonstrated that homogeneous layers of these nanospheres can be prepared by spin-coating the aqueous dispersion onto glass or silicon substrates. Most importantly, this miniemulsion process is well suited for an exact control of the nanosphere size between approximately 30 nm and 500 nm. It has also been shown that these layers can withstand high electrical current densities, and organic light-emitting diodes based on such layers exhibiting low onset voltages have been fabricated[19].

Here we demonstrate the application of the miniemulsion process to polymer blends, in which the dimension of phase separation can be precisely controlled by the diameter of the nanospheres. Two different approaches are presented, both using thin spin-coated layers (Fig. 1b). In the first approach, two dispersions of single-component nanospheres are mixed and processed into thin layers. In the second approach, the nanospheres are prepared from a mixture of two polymers in a suitable solvent. In this case, both polymers are contained in each individual nanoparticle, with the upper limit of the dimension of phase separation given by the particle size.

To demonstrate the applicability of these strategies, single-component and two-component particles were prepared from different semiconducting polymers (see Supplementary Information). Such polymers were chosen for several reasons. First, the fluorescence of conjugated polymers is known to be very sensitive to chemical and photophysical degradation processes, as well as to conformational changes[20–22]. Fluorescence studies on our blends will therefore be indicative of any significant changes of the polymers' electronic properties during layer processing. Second, these fluorescent polymers were selected to probe the morphology of the nanophase-separated structures using energy-transfer experiments.

For the first approach, dispersions were prepared from two fluorescent polymers: a solution-processable poly(*p*-phenylene)-type ladder polymer[23], m-LPPP, which does not show any softening up to the decomposition temperature of about 300–350 °C, and a derivative of polyfluorene, PF11112 (ref. 24), with the glass-transition temperature, T_g, close to room temperature (Fig. 2). The dispersions of the single-component nanoparticles were homogeneously mixed and spin-coated onto glass or silicon substrates. Figure 2a shows an atomic force microscopy (AFM) image of such an as-prepared layer. The resulting film consists of closely packed nanospheres, and the

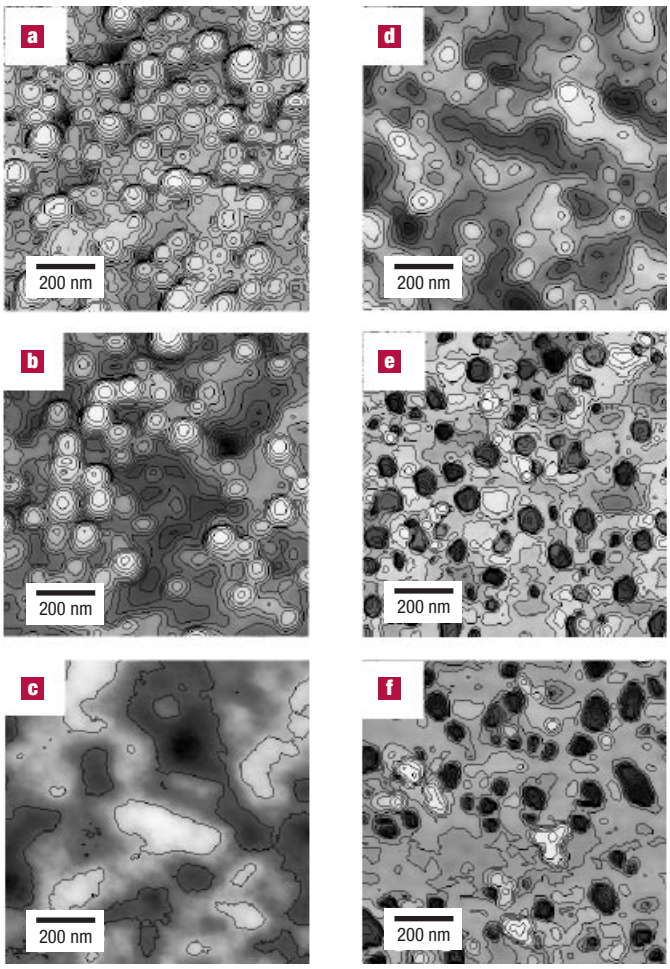

Figure 3 Thermal stability of the nanoscale phase-separation in layers of nanoparticle blends. AFM contour plot of a 1:1 mixture of particles of PF11112 (75 nm) and poly(methyl methacrylate) (PMMA) (80 nm). The images show plots recorded for: **a**, an as-prepared layer, **b**, a layer annealing at 75 °C, and **c**, a sample annealed at 150 °C. **d**–**f**, AFM images of the same layers after rinsing in acetone to dissolve the PMMA. The contour line spacing is about 8.5 nm.

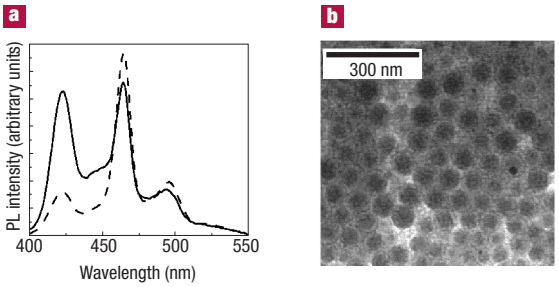

Figure 4 Energy transfer in two-component blend particles. a, Photoluminescence spectra of diluted dispersions of nanospheres containing both m-LPPP and poly(9,9-bis(2-ethylhexyl)fluorene-2,7-diyl) (PF2/6) at a weight ratio of 11. Data are shown for nanoparticle dispersions with a mean particle diameter of 64 nm (dashed line) and 149 nm (solid line). The excitation wavelength was 380 nm. **b**, Transmission electron microscope image of the two-component nanoparticles.

micrograph does not reveal any cracks within an area of $3 \times 3\ \mu m^2$. Obviously, some of the particles already coalesce on layer formation, which we assign to the low-T_g PF11112 nanospheres. After annealing at 150 °C for 1 h, the PF11112 particles appear to have coalesced to a rather homogeneous phase while the high-T_g m-LPPP nanospheres appear to be uniformly embedded within the continuous PF11112 layer (Fig. 2b). The sizes and heights of the m-LPPP particles as visible in the image are, however, larger than the average diameter of the m-LPPP particles, which we assign to the fact that the 'soft' PF11112 phase wets the 'hard' m-LPPP particles. On further annealing at 200 °C, the highly fluid PF11112 phase forms a smooth and continuous layer over almost the entire surface (not shown here), resulting in a large interfacial area between the two components.

These morphological changes are confirmed by energy-transfer experiments. Because the rate of energy transfer strongly depends on the distance between donor and acceptor moieties, this process has been extensively used to study the morphology of polymer blends[25,26]. Samples were optically excited at a wavelength of 380 nm, at which the PF11112 shows its maximum absorption but the m-LPPP absorption is only weak (see Fig. 2c and Supplementary Information). As shown by the fluorescence spectra in Fig. 2d, the emission is dominated by the m-LPPP emission peaks at 463 nm and 492 nm, indicating significant energy transfer from PF11112 to m-LPPP already in the as-prepared layer. On annealing at 200 °C, the PF11112 emission with the main peak at 422 nm is almost completely quenched whereas the m-LPPP emission has gained a fourfold intensity. At this stage, the PF11112 phase homogeneously surrounds the individual m-LPPP particles. In contrast, a layer containing only pure m-LPPP particles exhibited only very weak emission when measured under the same excitation conditions, proving that the m-LPPP emission of the mixed particle layer mainly involves energy transfer from the soft PF11112 phase. The absorption spectra shown in Fig. 2c further indicate that the polymers did not degrade on annealing. Finally, the observation that the decrease in PF11112 emission intensity is simultaneously accompanied by an increase of the m-LPPP emission is further proof that annealing does not lead to any significant changes in the electronic properties of one or both components.

It is important to note that even though the samples were annealed far above the T_g of the 'soft' PF11112 phase, we do not observe any agglomeration of the 'hard' m-LPPP particles. However, the question arises as to whether this nanoscale phase-separated morphology is stable even at a temperature above the softening point of both components. We have therefore investigated blends of particles of PF11112 and poly(methyl methacrylate) (PMMA). PMMA is particularly well suited because of its T_g of about 110 °C (which is above the T_g of PF11112 but well below the decomposition temperatures of both polymers) and its fair solubility in acetone (in which PF11112 is not soluble).

Figure 3 shows AFM contour plots of an as-prepared PF11112/PMMA (1:1 weight ratio) layer (Fig. 3a); a layer annealed at 75 °C (a temperature between the T_gs of PF11112 and PMMA; Fig. 3b) and a film annealed at 150 °C (Fig. 3c), above the softening temperature of both components. After the initial AFM measurements, these layers were washed in acetone to remove the PMMA exclusively (Fig. 3d–f). The contour plot of the as-prepared layer reveals an overall rough surface, with a full-width at half-maximum of the height distribution of 50 nm and an r.m.s. roughness of about 12 nm. After annealing at 75 °C, the individual PMMA particles become clearly resolved, extruding out of a rather structure-less PF11112 phase. The surface morphology changes drastically, however, when the layer is heated to 150 °C. Now, the whole surface appears to be smooth and featureless, with a low r.m.s.

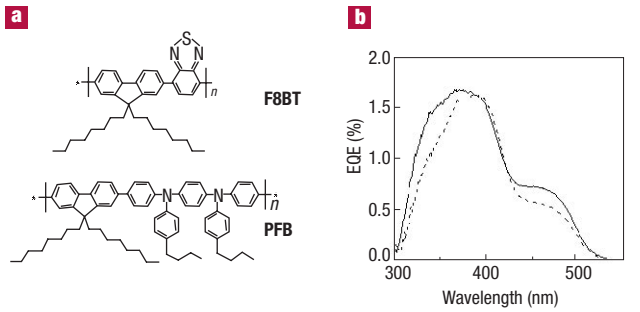

Figure 5 Solar cells based on two-component polymer nanoparticles. a, Chemical structure of the electron-accepting polymer poly(9,9-dioctylfluorene-co-benzothiadiazole (F8BT) and the hole-acceptor poly(9,9-dioctylfluorene-co-N,N-bis(4-butylphenyl)-N,N-diphenyl-1,4-phenylenediamine) (PFB). **b**, Spectrum of the external quantum efficiency (EQE) of single-layer solar cells fabricated from F8BT/PFB (1:1 weight ratio) blend particles, which were prepared using either xylene (solid line) or chloroform (dashed line) in the miniemulsion process.

roughness of only 4–5 nm; the AFM picture of the same layer after rinsing with acetone (Fig. 3f), shows that the underlying morphology is, nevertheless, structured on a nanometre scale. In fact, holes with widths ranging between about 80 and 150 nm and depths of 50–60 nm penetrate into the otherwise flat surface of the underlying PF11112 film. These holes (darker areas on Fig. 3f) are uniformly distributed throughout the whole layer surface, with an average next-neighbour distance of 90 nm. A similar morphology is already observed for the layer annealed at 75 °C. The resulting two-phase morphology of the sample annealed at 150 °C—above the softening temperature of both polymers—can be described by a bilayer structure, with the PMMA phase forming the top layer, but with channels about 80–150 nm wide protruding into the underlying PF11112 film. This domain structure resembles those of certain polymer blends formed on spin-coating from organic solvents onto suitable substrates, for example, blends of polystyrene and PMMA spin-coated from tetrahydrofuran on SiO_x; however in this case, the size of the lateral domains is in the micrometre range[7]. We presume that the vertically interdigitated nanoscale morphology is a result of several processes. First, the subsequent softening of the two polymers (due to the different glass transitions) lead to an intermediate structure in which hard PMMA particles are immersed in a continuous PF11112 bottom layer. Second, softening of the PMMA will result in the formation of a continuous PMMA top layer, but at the same time the interaction between the more polar PMMA phase and the polar glass surface stabilizes the existing PMMA channels within the PF11112 bottom layer. Further experiments need to be performed to reveal the role of substrate polarity on the stability of these two-component morphologies. Nevertheless, the results presented here demonstrate that the nanoparticle approach allows for the preparation of novel nanoscale domain structures in thin polymer films, and that these structures are fairly stable even at temperatures above the glass transitions of both polymer components.

In the second approach, miniemulsions were prepared starting from a solution containing two polymers. We expected that after evaporation of the solvent, the resulting nanoparticle dispersion would contain a blend of both polymers inside each individual nanoparticle. As an example, a dispersion prepared from a solution of a high-T_g polyfluorene derivative, poly(9,9-bis(2-ethylhexyl)fluorene-2,7-diyl), PF2/6, and m-LPPP (at a 1:1 weight ratio) was studied by energy-transfer experiments. As shown by the transmission electron microscope image of Fig. 4, these particles have a spherical shape, with only a small variation in size. Figure 4 shows the photoluminescence spectra (excited at 380 nm) of two highly diluted dispersions containing nanospheres with mean diameters of 64 nm and 149 nm, respectively. The relative peak ratio of the m-LPPP emission at 463 nm compared with the PF2/6 emission at 422 nm is about 1.1: 1 for the particles with 149 nm diameter and 4.4:1 for the 69 nm particles. The significant m-LPPP emission on excitation at 380 nm clearly indicates that each particle contains a blend of both polymers. Further, photoluminescence spectra were measured at different particle concentrations, down to about 10^{-5} wt% (see Supplementary Information), to ensure that the m-LPPP emission is not caused by the generation and re-absorption of PF2/6 fluorescent light in different particles. Further, the observation that the m-LPPP emission is larger for the smaller particles leads us to the conclusion that the two polymers are not homogeneously mixed within the nanospheres. Even though we have not further studied the process of particle formation, we presume that phase separation inside the particles occurs at the stage of solvent extraction, with the domain size controlled mainly by the diameter of the particles.

We applied the nanoparticle concept to prepare optoelectronic devices with controlled nanophase morphology of the active layer. We have investigated organic solar cells made from the hole-accepting polymer PFB and the electron acceptor F8BT (Fig. 5). These polymers have been chosen because the morphologies and domain dimensions of blends of PFB and F8BT, and also the properties of solar cells using PFB/F8BT blend layers, were shown to depend strongly on the choice of solvent and on the deposition conditions[9,27,28]. Single-layer solar cells using PFB/F8BT (1:1) blend layers spin-coated from xylene yielded external quantum efficiencies between 0.25 and 1.5%[9,27], depending on substrate temperature and coating conditions, whereas solar cells prepared from chloroform exhibited efficiencies of up to 4%[27]. We fabricated nanospheres from a 1:1 by weight mixture of PBT and F8BT using either xylene or chloroform as the solvent in the miniemulsion process. The resulting solid two-component particles had mean diameters of 49 nm and 53 nm, respectively. Solar cells were fabricated by spin-coating the aqueous dispersion onto glass covered with a transparent indium tin oxide electrode. The device was completed by evaporating a Ca/Al cathode onto the particle monolayer. Figure 5 shows the external quantum efficiency of these devices as a function of wavelength for an incident intensity of about 1 mW cm^{-2}. Most importantly, the quantum efficiencies of the devices prepared with both types of particles are comparable, with a peak value of about 1.7%. This suggests that the solar-cell properties were entirely controlled by the size of the two-component particle. Moreover, since the solar-cell efficiency was almost not affected by the choice of solvent used in the miniemulsion process, we conclude that the dimension of phase separation in these layers is indeed determined by the particle diameter. The efficiencies of our solar cells are among the best reported for solar cells using 1:1 PBT/F8BT layers spin-coated from xylene, but still below the efficiencies reported for layers deposited from chloroform[27]. Further work with respect to the optimization of the blend composition and the particle size are the subject of current research.

Finally, we acknowledge that single-component polymer nanoparticles, as well as two-component polymer nanoparticles with core–shell morphologies, can be prepared by emulsion polymerization[29,30]. However, this type of heterophase polymerization is limited to the radical polymerization of barely water-soluble monomers such as methacrylates or styrene. Further, several micrometre-thick polymer-blend latex layers of two types of particles have been studied[31,32], but to our knowledge, no investigations on submicrometre-thick layers of particle blends or even particle-blend monolayers have been reported. Polymer nanoparticles can also be obtained by the process of miniemulsion polymerization. In this case, small, homogeneous and stable droplets of suitable precursors are directly reacted to the final polymer dispersion. Here, a larger variety of

monomers can be used, because polymerization in miniemulsions is not only limited to radical polymerization[33]. However, no heterophase polymerization or polycondensation has yet been applied to functional polymers. A major drawback of this approach to functional polymers is that the resulting polymerization product cannot be purified, and catalyst as well as ionic and low-molecular-weight impurities will remain embedded in the solid polymer nanoparticles.

In conclusion, we have prepared layers of polymer beads with well-defined dimensions of phase separation using single-component and multicomponent polymer nanoparticles. Even though the results presented here were obtained for spin-coated layers, it should be possible to use these nanoparticles to fabricate multicomponent bulk samples. In contrast with approaches published earlier, our strategy to nanostructured polymer blends does not require any chemical modification of the polymer structure. Moreover, it should be applicable to virtually any material that is soluble in an organic solvent (immiscible with water), and which forms a solid phase after solvent extraction. We have also shown that the efficiencies of solar cells using our two-component particles are comparable to those of devices prepared from solution at comparable illumination conditions, and that they are not affected by the choice of solvent used in the miniemulsion process.

Further work will be devoted to the study of the formation and stability of nanophase structures, with special focus on the formation of bicontinuous morphologies. Furthermore, the preparation and optimization of optoelectronic devices such as nano-sized light-emitting diodes and solar cells will be subject of future work.

Received 23 October 2002; accepted 28 March 2003; published 11 May 2003.

References

1. Halls, J. J. M. *et al.* Efficient photodiodes from interpenetrating polymer networks. *Nature* **376,** 498–500 (1995).
2. Yu, G., Gao, J., Hummelen, J. C., Wudl, F. & Heeger, A. J. Polymer photovoltaic cells — enhanced efficiencies via a network of internal donor-acceptor heterojunctions. *Science* **270,** 1789–1791 (1995).
3. Brabec, C. J., Sariciftci, N. S. & Hummelen, J. C. Plastic solar cells. *Adv. Funct. Mater.* **11,** 15–26 (2001).
4. Jones, R. A. L., Norton, L. J., Kramer, E. J., Bates, F. S. & Wiltzius, P. Surface-directed spinodal decomposition. *Phys. Rev. Lett.* **66,** 1326–1329 (1991).
5. Böltau, M., Walheim, S., Mlynek, J., Krausch, G. & Steiner, U. Surface-induced structure formation of polymer blends on patterned substrates. *Nature* **391,** 877–879 (1998).
6. Krausch, G. Surface-induced self-assembly in thin polymer films. *Mater. Sci. Eng. R* **14,** 1–94 (1995).
7. Walheim, S., Böltau, M., Mlynek, J., Krausch, G. & Steiner, U. Structure formation via polymer demixing in spin-cast films. *Macromolecules* **30,** 4995–5003 (1997).
8. Müller-Buschbaum, P., Gutmann, J. S. & Stamm, M. Influence of blend composition on phase separation and dewetting of thin polymer blend films. *Macromolecules* **33,** 4886–4895 (2000).
9. Halls, J. J. M. *et al.* Photodiodes based on polyfluorene composites: Influence of morphology. *Adv. Mater.* **12,** 498–502 (2000).
10. Shaheen, S. E. *et al.* 2.5% efficient organic plastic solar cells. *Appl. Phys. Lett.* **78,** 841–843 (2001).
11. Hamley, I. W. *The Physics of Copolymers* (Oxford Univ. Press, New York, 1998).
12. Binder, K. in *Polymers in Confined Environments* (ed. Granick, S.) 1–89 (Advances in Polymer Science Series **138,** Springer, Berlin, 1999).
13. Schmitt, C., Nothofer, H.-G., Falcou, A. & Scherf, U. Conjugated polyfluorene/polyaniline block copolymers. *Macromol. Rapid. Commun.* **22,** 624–628 (2001).
14. Johansson, D. M., Theander, M., Granlund, T., Inganäs, O. & Anderson, M. R. Synthesis and characterization of polyfluorenes with light-emitting segments. *Macromolecules* **34,** 1981–1986 (2001).
15. Macosko, C. W. *et al.* Compatibilizers for melt blending: Premade block copolymers. *Macromolecules* **29,** 5590–5598 (1996).
16. Hillmyer, M. A., Maurer, W. W., Lodge, T. P., Bates, F. S. & Almdal, K. Polymeric co-continuous microemulsions in ternary homopolymer/block copolmer blends. *J. Phys. Chem. B* **103,** 4814–4824 (1999).
17. Pernot, H., Baumert, M., Court, F. & Leibler, L. Design and properties of co-continuous nanostructured polymers by reactive blending. *Nature Mater.* **1,** 54–58 (2002).
18. Landfester, K. *et al.* Semiconducting polymer nanospheres in aqueous dispersion prepared by a miniemulsion process. *Adv. Mater.* **14,** 651–655 (2002).
19. Piok, T. *et al.* Organic light-emitting devices fabricated from semiconducting nanospheres. *Adv. Mater.* (in the press).
20. Yan, M., Rothberg, L. J., Papadimitrakopoulos, F., Galvin, M. E. & Miller, T. M. Defect quenching of conjugated polymer luminescence. *Phys. Rev. Lett.* **73,** 744–747 (1994).
21. Bliznyuk, V. N. *et al.* Electrical and photoinduced degradation of polyfluorene based films and light-emitting devices. *Macromolecules* **32,** 361–369 (1999).
22. Grell, M., Bradley, D. D. C., Ungar, G., Hill, J. & Whitehead, K. S. Interplay of physical structure and photophysics for a liquid crystalline polyfluorene. *Macromolecules* **32,** 5810–5817 (1999).
23. Scherf, U. & Müllen, K. Polyarylenes and poly(arylenevinylenes). 7. A soluble ladder polymer via bridging of functionalized poly(para-phenylene)-precursors. *Macromol. Chem. Rapid Commun.* **12,** 489–497 (1991).
24. Scherf, U. & List, E. J. W. Semiconducting polyfluorenes: Towards reliable structure-property relationships. *Adv. Mater.* **14,** 477–487 (2002).
25. Zhao, Y., Levesque, J., Roberge, P. C. & Prudhomme, R. E. A study of polymer blends by nonradiative energy-transfer fluorescence spectroscopy. *J. Polym. Sci. Polym. Phys.* **27,** 1955–1970 (1989).
26. Jiang, M., Chen, W. J. & Yu, T. Y. Controllable specific interactions and miscibility in polymer blends. 3. Nonradiative energy-transfer fluorescence studies. *Polymer* **32,** 984–989 (1991).
27. Arias, A. C. *et al.* Photovoltaic performance and morphology of polyfluorene blends: A combined microscopic and photovoltaic investigation. *Macromolecules* **34,** 6005–6013 (2001).
28. Snaith, H. J., Arias, A. C., Morteani, A. C., Silva, C. & Friend, R. H. Charge generation kinetics and transport mechanisms in blended polyfluorene photovoltaic devices. *Nanoletters* **2,** 1353–1357 (2002).
29. Winnik, M. A. Latex film formation. *Curr. Opin. Colloid Interface Sci.* **2,** 192–199 (1997).
30. Blackley, D. C. *Polymer Latices* (Chapman & Hall, London, 1997).
31. Patel, A. A., Feng, J. R., Winnik, M. A., Vancso, G. J. & McBain, C. B. D. Characterization of latex blend films by atomic force microscopy. *Polymer* **37,** 5577–5582 (1996).
32. Feng, J. R., Winnik, M. A., Shivers, R. R. & Clubb, B. Polymer blend latex films — morphology and transparency. *Macromolecules* **28,** 7671–7682 (1995).
33. Landfester, K. Polyreactions in miniemulsions. *Macromol. Rapid Commun.* **22,** 896–936 (2001).

Acknowledgements

We would like to thank W. Regenstein (University of Potsdam) for the access to the optical spectrometers used in this work, A. Heilig (MPI of Colloids and Interfaces) for performing the AFM measurements and M. Förster (University of Wuppertal) for experimental support in the polymer synthesis. We also acknowledge financial support by the Stiftung Volkswagenwerk and the Max-Planck Society.

Correspondence and requests for materials should be addressed to D.N., K.L. or U.S.

Supplementary Information is available on the *Nature Materials* website (http://www.nature.com/naturematerials).

Competing financial interests

The authors declare that they have no competing financial interests.

SYNTHESIS OF THE AQUEOUS POLYMER DISPERSIONS:

The miniemulsions of single component nanoparticles were prepared as described in a previous paper (Landfester, K. et al. *Semiconducting Polymer Nanospheres in Aqueous Dispersion Prepared by a Miniemulsion Process.* Advanced Materials **14**, 651-655 (2002)).

For the preparation of the two-component particles, 20 mg of m-LPPP and 20 mg of PF2/6 were dissolved in 2.3 g (to obtain 150 nm particles) or 4.3 g (to obtain 64 nm particles) of chloroform. Each polymer solution was then mixed with 10 g of an aqueous SDS solution (2.4 wt.% related to the amount of chloroform) and stirred for 1 h for pre-emulsification. The miniemulsion was prepared by ultrasonicating the mixture for 2 min at 70 % amplitude (Branson sonifier W450) using a microtip. After sonication the sample was stirred at 62 ºC in order to evaporate the organic solvent. Finally, the dispersion was dialysed to decrease the amount of SDS to about 5 wt.% with respect to the polymer. Particles containing PFB and F8BT (purchased from ADS) were prepared following the same route, utilizing either xylene or chloroform as solvent. Table 1 summarizes the characteristics of the different dispersions used for our investigations.

Table 1: Dispersions of single- and two-component nanoparticles with a 1:1 weight ratio.

POLYMER 1	POLYMER 2	PARTICLE SIZE (nm)
m-LPPP	-	95
PF11112	-	74
PMMA	-	80
PF2/6	m-LPPP	149
PF2/6	m-LPPP	64
PFB	F8BT	53 (using $CHCl_3$)
PFB	F8BT	49 (using C_3H_6O)

ANALYSIS:

The particle sizes were measured using a Nicomp particle sizer (Model 370, PSS Santa Barbara, USA) at a fixed scattering angle of 90 °. Atomic force microscopy (AFM) was performed with a NanoScope IIIa microscope (Digital Instruments, Santa Barbara) operating in tapping mode. The instrument was equipped with a 10 x 10 micrometer E-Scanner and commercial silicon tips (model TSEP, the force constant was 50 $N \cdot m^{-1}$, the resonance frequency was 300 kHz and the tip radius was smaller than 20 nm).

Absorption spectra were measured with a Perkin Elmer Lambda 19 UV/Vis spectrometer. The spectrum of the sample was corrected for the transmission of an uncoated glass slide.

Fluorescence spectra were recorded with a Perkin Elmer LS 50 luminescence spectrometer. The excitation was incident at an angle of 60 ° onto the front face of the sample and the emission was recorded in reflection at an angle of 30 ° with respect to the surface normal.

FILM PREPARATION:

Glass substrates were cleaned with a standard procedure involving a ultrasonic bath in a soap solution followed by thoroughly washing steps with deionisized water. Films were prepared by dropping ca. 80 µl of the miniemulsion on a rotating glass substrate (spinning speed in the range of 3000-4200 rpm). Annealing of the samples was performed either in a vacuum oven or on a hot plate in a glove box under nitrogen atmosphere. It is known from literature that the quality of the nanosphere layers prepared from aqueous dispersions depends strongly on the wetting of the substrate, the spinning speed and the particle concentration (Deckman, H. W., Dunsmuir, J. H., Garoff, S., McHenry, J. A. & Peiffer, D. G. *Macromolecular self-organized assemblies.* J. Vac. Sci. Technol. B **6**, 333–336 (1988); Anczykowski, B., Chi, L. F. & Fuchs, H. *Atomic-Force Microscopy Investigations on Polymer Latex Films.* Surf. Interface Anal. **23**, 416–425 (1995)). The best results were obtained with plasma cleaned substrates, spinning speeds in the range of 3000-5000 rpm and particle concentrations of 4-6 wt.%.

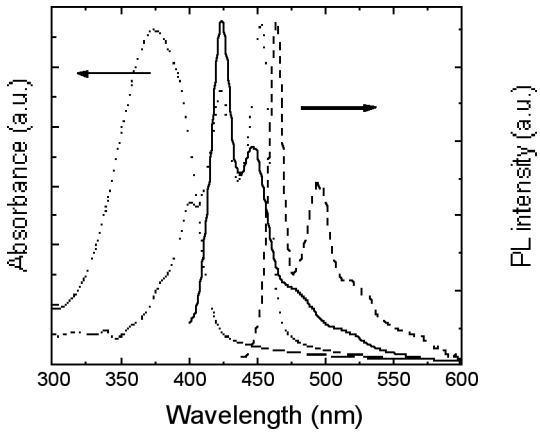

Absorption and emission spectra of PF11112 and m-LPPP:

Absorption (symbols) and photoluminescence (lines) spectra of a layer of m-LPPP particles (solid symbols and solid line) or of PF2/6 particles (open symbols and dashed line) deposited on glass.

SUPPLEMENTARY INFORMATION

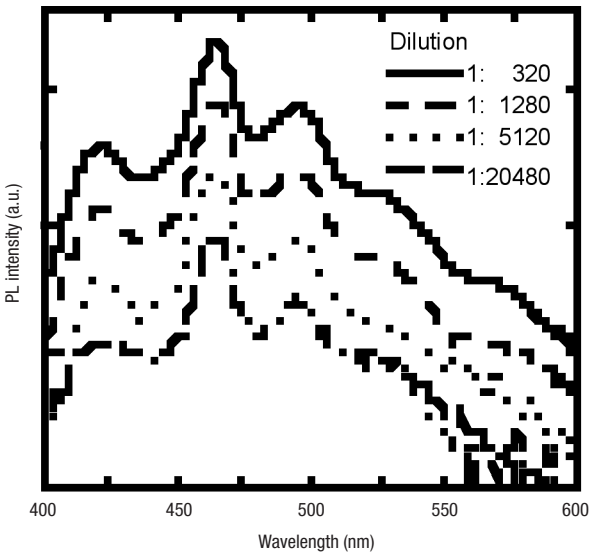

Absorption spectra of diluted dispersions of nanoparticles containing PF2/6 and m-LPPP:

PL spectra of diluted dispersions of nanoparticles containing both PF2/6 and m-LPPP with a mean particle diameter ca. 64 nm. The non-diluted dispersion had a solid content of 0.5 wt.%. The dispersions were diluted with MilliQ water.

PREPARATION AND CHARACTERIZATION OF SOLAR CELLS:

Nanoparticles composed of F8BT:PFB (1:1 weight ratio) were spincoated onto substrates covered with a 100 nm thick layer of indium tin oxide. After drying a cathode consisting of a ca. 20 nm layer of calcium and a 100 nm thick layer of aluminum was deposited on top in a Leybold thermal evaporator at a base pressure of $1\text{-}2\times10^{-6}$ mbar. For the measurement of the external quantum efficiency the device was illuminated through the ITO substrate with a fused silica fiber. The incident light intensity was ca. 1 mW/cm^2. The preparation and device characterization was performed in inert gas atmosphere.